IOP Conf. Series: Materials Science and Engineering **396** (2018) 012049 doi:10.1088/1757-899X/396/1/012049

Load harmonics extraction based decoupled control of grid connected solar photovoltaic system

Fossy Mary Chacko[1*], Jayan M V[2] and Prince A[3]

[1*]Research Scholar, [2]Professor and [3]Associate Professor, Department of Electrical Engineering, Rajiv Gandhi Institute of Technology, Kottayam, Kerala, India
E-mail*: marynbiji@gmail.com

Abstract. The global energy shortage and the requirement for energy systems that are sustainable has led to the widespread penetration of Renewable Energy Sources (RES). The intermittent characteristics of these Renewable Energy Sources make it a daunting task to integrate renewable energy, especially solar energy resources into the electric grid. The increasing number of Distributed Generation (DG) systems along with the existing non-linear loads create several issues due to variable output power and further worsens power quality problems like overvoltage, voltage fluctuations and harmonics. This paper describes an attempt on the development of a control strategy based on decoupled control with load harmonics extraction for the mitigation of power quality issues in grid integrated Solar Photovoltaic (SPV) systems. The performance of the grid integrated SPV system with linear and non-linear loads is investigated by simulation using MATLAB/Simulink. The effectiveness of the developed control strategy is validated by comparing the performance with an uncompensated system consisting of grid with linear and non-linear loads.

Keywords: Distributed Generation, Power Quality, Solar Photovoltaic (SPV)

1. Introduction

The global energy crisis and the need for sustainable energy systems has paved way for the development of power supply structures that are based mainly on renewable resources. The high penetration of RES requires new strategies for the operation and grid management in order to maintain or even to improve the electric power supply reliability and quality [1]. This paper focuses on the SPV system which is now gaining increased importance as a Renewable Energy (RE) source owing to advantages such as inexhaustibleness, the absence of fuel cost and harmful emissions, reduced maintenance and less wear and tear. The intermittent nature of RES makes it a challenging task to integrate renewable energy, especially solar energy resources into the power grid [2]. The increasing number of SPV systems imposes several issues [3] like variable output power, power quality problems, islanding, storage and compliance to standards. The integration of Photo Voltaic (PV) systems in low voltage distribution systems has led to the introduction of power quality problems like overvoltage, voltage fluctuations and harmonics. Moreover, the output power being fed to the grid depends on the existing conditions of insolation and temperature. This situation combined with the existing non-linear loads at the Point of Common Coupling (PCC) further deteriorates the power quality. There exist several solutions to the power quality problems like traditional passive filters, active filters and hybrid filters [4]. Distribution STATic COMpensators (DSTATCOMs) based on Voltage

Source Inverter (VSI) have become popular to reduce the problems associated with the ac distribution system, such as reactive power compensation, load balancing, and harmonic current elimination [5]. In this work, a control strategy based on decoupled control with load harmonics extraction for the PV inverter is developed for the amelioration of power quality issues in grid integrated SPV systems. The effectiveness of the proposed control strategy is validated by comparing the performance with an uncompensated system. The paper is organized as follows. Firstly, Section 2 briefly describes the grid connected PV system configuration. The modeling of PV array and the detailed design of the various components of the grid connected PV system is presented in Section 3. The proposed load harmonics extraction based decoupled control strategy is illustrated in Section 4. Section 5 presents the simulation results. Finally, the conclusions are given in Section 6.

2. System Description

PV systems can be mainly categorized as Stand-alone, Grid-connected and Hybrid PV systems [6]. A stand-alone system is the one which is not connected to the power grid. The PV systems integrated to the grid are called grid-connected PV systems. Hybrid PV systems may be of stand-alone or grid-connected type, but have at least one other power source other than PV. The major difference between the grid-connected and stand-alone systems comes from the energy storage feature. While the stand-alone PV systems usually have a provision for energy storage, the grid-connected PV systems have none. This research work focuses on the grid integrated PV System. The Block Diagram representation of a typical grid connected PV System is shown in figure 1.

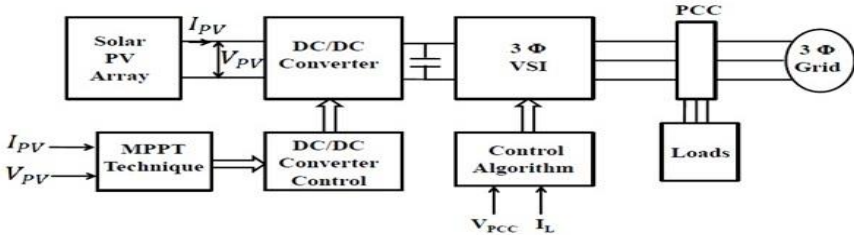

Figure 1. Grid connected PV system configuration

The grid interfaced solar PV generating system consists of a Solar PV Array, DC-DC boost conversion stage and a current controlled VSI interfaced to three-phase ac grid [7]. The output power from the Solar PV array is fed to a DC-DC boost converter stage in order to boost the PV array voltage to the required DC bus voltage level of VSI. Thus the active power generated by the SPV array is fed to the common DC link. The intermittent nature of the solar energy resource necessitates the use of Maximum Power Point Tracking (MPPT) [8]. In this paper, the Perturb and Observe (P & O) method is adopted to extract maximum power from the SPV array under different conditions of insolation.

3. Design of grid-connected SPV system

The system consisting of PV array and VSI is interfaced with a relatively large ac system, i.e. a stiff utility grid of 415 V. The operating frequency is dictated by the ac system and is fairly constant. The design of the various stages of the grid integrated SPV system [9] is given as follows:

3.1. SPV array design

The modelling of PV Array is based on the Single Diode Model (SDM) of PV cell [10]. The Light generated current for any operating conditions of the PV array is related to the photocurrent at Standard Test Conditions (STC) as: $I_{PV} = \left[I_{SC,n} + K_I(T - T_n)\right]\left(\frac{G}{G_n}\right)$ (1)

where, $I_{SC,n}$= light generated current at nominal temperature and irradiance, K_I = short circuit current temperature co-efficient, T = temperature of the p-n junction in Kelvin, T_n= nominal temperature = 273 K, G = solar insolation in W/m^2, G_n = solar insolation at STC= 1000 W/m^2

For a SPV array with N_S modules in series and N_P modules in parallel, the output current equation is defined as: $I = I_{PV}\, N_P - N_P I_O \left[exp\left(\frac{(V+R_S I)}{N_S V_t aC}\right) - 1\right] - \left(\frac{V+R_S I}{R_P}\right)$ (2)

where, I_O = reverse saturation current, V_t= thermal voltage of solar cell, a = Diode ideality factor, C = Number of cells connected in series in a module, R_S = equivalent series resistance of the array, R_P = equivalent parallel resistance of the array. The parameters of PV array model used for simulation are given in table 1. The SPV array is designed to generate a maximum power of 25 kW with input voltage to the boost converter V_{boost} in the range of 500 V. Here, the open circuit voltage of module V_{oc} is 32.9 V, and current at maximum power point I_{mp} is 7.61 A. The number of PV modules to be connected in series and parallel are given by:

$$N_s = \frac{V_{boost}}{V_{oc}} = 15.19 \text{ or } 16 \text{ modules and } N_p = \frac{{}^{P_{max}}/_{N_s V_{oc}}}{I_{mp}} = 6.24 \text{ or } 7 \text{ modules} \quad (3)$$

3.2. Design and selection of DC link voltage V_{dc}

The minimum value of DC bus voltage for VSI must be selected such that it is twice the value of peak phase voltage at the PCC: $V_{dc} = \frac{2\sqrt{2}V_L}{\sqrt{3}m} = 677.7\ V$ (4)

where, V_L = Line Voltage of the grid, m = Modulation index= 1. The DC link voltage is selected as 700 V.

3.3. Design of VSI DC Link Capacitance

The VSI DC Link Capacitance value is determined as: $C_{dc} = \frac{{}^{P_{dc}}/_{V_{dc}}}{2\omega V_{dc,ripple}} = 4062\ \mu F$ (5). Where, P_{dc} is the power available at the dc link and ω is the angular frequency. The % Ripple in dc link voltage $V_{dc,ripple}$ is taken as 2% of V_{dc}. The value of VSI DC link capacitance is selected as 4000 μF.

3.4. Design of Coupling Inductances

The value of the coupling ac inductor is computed as: $L_f = \frac{\sqrt{3}\,mV_{dc}}{12hf_s\Delta i} = 7.86\ mH \cong 8\ mH$ (6)

Where, h =overloading factor = 1.2, f_s =Switching frequency, Δi = Ripple current which is assumed to be 3% of the peak current.

3.5. Design of Boost Converter

A two stage grid connected PV system is designed here. The intermediate dc-dc converter is in the unidirectional boost topology that boosts the output voltage from the Solar PV array V_{PV} and feeds the active power generated to the DC Bus of the VSI at a voltage V_{dc}. The boost converter consists of the energy storage reactor L_b, switch S, diode D and output capacitor C_b. The boost converter voltage relation is given by : $V_{dc} = {}^{V_{PV}}/_{1-D}$ (7). The energy storage reactor L_b is designed for a switch Duty Ratio of 0.25, switching frequency f_{sw} of 10 kHz and input current ripple of 3% as: $L_b = \frac{V_{dc}D(1-D)}{2f_{sw}\Delta i_{in}}$ (8). The DC link capacitance C_{dc} serves as the output capacitor C_b of the boost converter stage. The boost converter is linked to the PV system with a filter capacitor C_1 for decreasing the ripple caused by the high frequency switching of switch S. The designed parameters of grid-connected SPV system used for simulation are given in table 2.

Table 1. PV Array parameters.

Array Parameters	
R_S: 0.23 Ω	a:1.3
R_p: 600 Ω	$I_{SC,n}$: 8.21 A
V_t: 0.0257	K_I: 3.2 x 10^{-3}
C:54	T_n: 273 K

Table 2. Parameters of grid-connected SPV System.

Grid-connected SPV system Parameters	
N_S: 16	L_f: 8 mH
N_P: 7	f_s: 10 kHz
V_{dc}: 700 V	L_b: 4.59 mH
C_{dc}: 4000 μF	C_b: 4000 μF

4. Proposed Control Strategy: Load Harmonics Extraction Based Decoupled Control

The flexibility and reliability of the grid integrated SPV system depends on the control algorithm employed for the switching of the PV inverter. The control scheme is based on the concepts of instantaneous power in the synchronously rotating d-q reference frame. The rotating reference frame is employed in this work because it offers higher accuracy compared to stationary frame based techniques. The PV inverter can be modeled [11] as follows in the synchronously rotating reference frame (d-q frame). Here, the inverter output emfs are represented as V_{invd}, V_{invq} and the grid voltages are represented as V_{gd},V_{gq}.

$$p\begin{bmatrix} i_d \\ i_q \end{bmatrix} = \begin{bmatrix} \frac{-R_s}{L_s} & \omega \\ -\omega & \frac{-R_s}{L_s} \end{bmatrix}\begin{bmatrix} i_d \\ i_q \end{bmatrix} + \frac{1}{L_s}\begin{bmatrix} V_{invd} - V_{gd} \\ V_{invq} - V_{gq} \end{bmatrix} \tag{9}$$

The new co-ordinate system is defined with the d-axis always coincident with the instantaneous grid voltage vector. Thus in the d-q frame, the q-axis component of the grid or source voltage is zero i.e. $V_{gq} = 0$.

$$p\begin{bmatrix} i_d \\ i_q \end{bmatrix} = \begin{bmatrix} \frac{-R_s}{L_s} & \omega \\ -\omega & \frac{-R_s}{L_s} \end{bmatrix}\begin{bmatrix} i_d \\ i_q \end{bmatrix} + \frac{1}{L_s}\begin{bmatrix} V_{invd} - V_{gd} \\ V_{invq} \end{bmatrix} \tag{10}$$

4.1. Decoupled control of i_d and i_q

Inspection of equation (10) leads directly to a rule that will provide decoupled control of i_d and i_q. The inverter voltage vector is controlled as follows:

$$V_{invd} = L_s(x_1 - \omega i_q) + V_{gd}$$
$$V_{invq} = L_s(x_2 + \omega i_d) \tag{11}$$

Substitution of equation (11) in equation (10) gives rise to the following relation:

$$p\begin{bmatrix} i_d \\ i_q \end{bmatrix} = \begin{bmatrix} \frac{-R_s}{L_s} & 0 \\ 0 & \frac{-R_s}{L_s} \end{bmatrix}\begin{bmatrix} i_d \\ i_q \end{bmatrix} + \begin{bmatrix} x_1 \\ x_2 \end{bmatrix} \tag{12}$$

Equation (12) shows that i_d and i_q respond to x_1 and x_2 respectively through a simple first order transfer function with no cross coupling. The control rule of inverter voltage equations is completed by defining feedback loops of Proportional and Integral (PI) compensators PI_1 (with proportional gain $K_1$and integral gain K_2) and PI_2 (with proportional gain K_3 and integral gain K_4) as follows:

$$x_1 = \left(K_1 + \frac{K_2}{s}\right)\left(i_{dref} - i_d\right) \tag{13}$$

$$x_2 = \left(K_3 + \frac{K_4}{s}\right)\left(i_{qref} - i_q\right) \tag{14}$$

4.2. Detection Algorithm based on Load Harmonics Extraction

One of the important aspects in the control scheme design is the detection algorithm used for determining the compensating current and voltage references. The effectiveness of the VSI for compensation depends on the method implemented to generate the reference template. The compensating current reference for the PV inverter consists of d and q axis components i_{dref} and i_{qref}. The compensating current reference template is derived from the load currents. The load currents are sensed and transformed from abc to dq frame, namely i_{ld} , i_{lq}. The d-axis component of compensating current reference for the PV inverter consists of two parts: (i) The d-axis component of load current harmonics i_{ldh} which is extracted as follows. The fundamental d-axis component of load current i_{ldf} is first extracted using a Low Pass Filter. Then, the d-axis component of load current harmonics i_{ldh} is obtained by subtracting this fundamental component from the d-axis component of load current i_{ld}. (ii) The current necessary for regulating the dc bus voltage to the desired level. This current is denoted as Δi_d and its amplitude is determined by the dc bus voltage regulation loop. Thus,

the real power can be regulated by varying i_{dref} in response to the error in the dc link voltage via PI compensator PI_3 (with proportional gain K_5 and integral gain K_6). The q-axis component of compensating current reference for the PV inverter consists of the q-axis component of the load current i_{lq}. Thus, the PV inverter is designed to inject the entire reactive power requirement of the load. The compensating current reference template for the PV inverter is thus given by:

$$i_{dref} = i_{ldh} + \Delta i_d = i_{ldh} + \left(K_5 + \frac{K_6}{s}\right)\left(V_{dcref} - V_{dc}\right) \quad (15)$$

Where, V_{dcref} is the reference value of dc link voltage.

$$i_{qref} = i_{lq} \quad (16)$$

The compensating current references are then compared with the actual inverter currents as shown in figure 2. The inverter output voltages can be expressed in terms of the dc link voltage and switching function matrix as: $\begin{bmatrix} V_{invd} \\ V_{invq} \end{bmatrix} = \frac{1}{2} maV_{dc} \begin{bmatrix} S_d \\ S_q \end{bmatrix}$ (17). For modulation index m and turns ratio a of 1, equation (17) becomes: $\begin{bmatrix} V_{invd} \\ V_{invq} \end{bmatrix} = \frac{V_{dc}}{2} \begin{bmatrix} S_d \\ S_q \end{bmatrix}$ (18). Thus, $\begin{bmatrix} S_d \\ S_q \end{bmatrix} = \frac{2}{V_{dc}} \begin{bmatrix} V_{invd} \\ V_{invq} \end{bmatrix}$ (19).

The switching function matrix in dq frame is transformed back to abc frame. The modulating signals S_{abc} are compared with triangular carrier signals (10 kHz) to obtain the PWM gating pulses for switches S_1 to S_6 of the PV inverter.

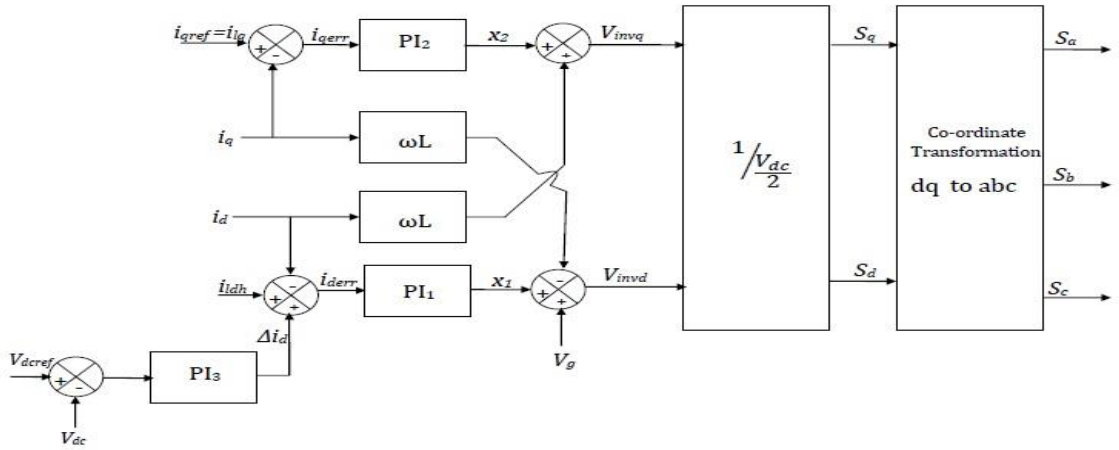

Figure 2. Structure of load harmonics extraction based decoupled control strategy of PV inverter

5. Simulation Results

The uncompensated system is initially simulated and the performance of the compensated two-stage three phase grid connected SPV system with linear and non-linear loads at PCC is then investigated using MATLAB/Simulink. In the compensated system, the PV inverter functions as a virtual DSTATCOM. Decoupled control with load harmonics extraction is employed as the control strategy for the current mode control of PV inverter. In both cases, an 18 kVA reactive load is connected at the PCC from 0 to 0.25 s. From 0.25 s to 0.5 s, a three phase 14 kVA non-linear diode rectifier load and 6 kVA reactive load are connected at the PCC.

5.1. Uncompensated System

The uncompensated system consists of three phase utility grid with linear and non-linear loads at the PCC. Figure 3 depicts the grid and the load voltage and current waveforms under the changing load conditions. It can be seen that distorted load currents cause distortion in the grid side currents. Also, the grid power factor is lagging. Figure 4 depicts the grid and the load real and reactive power. It can be observed that the entire real and reactive power requirement of the load is met by the utility grid.

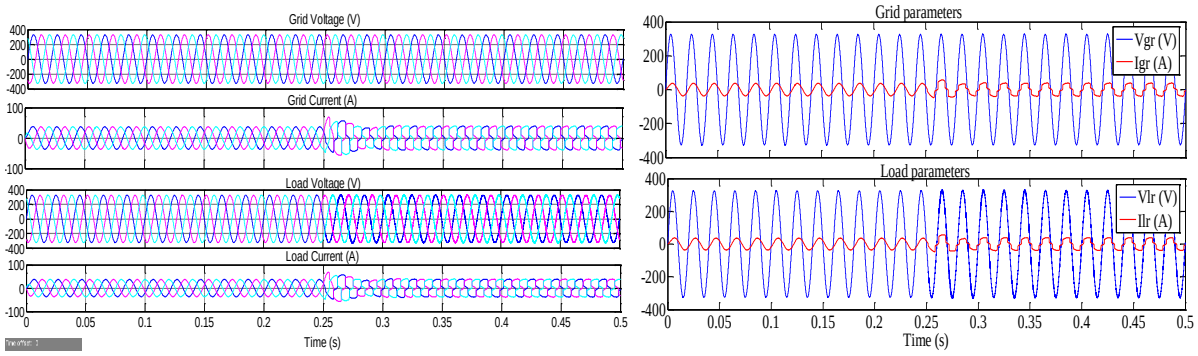

(a) (b)

Figure 3. Response of uncompensated system under changing load conditions

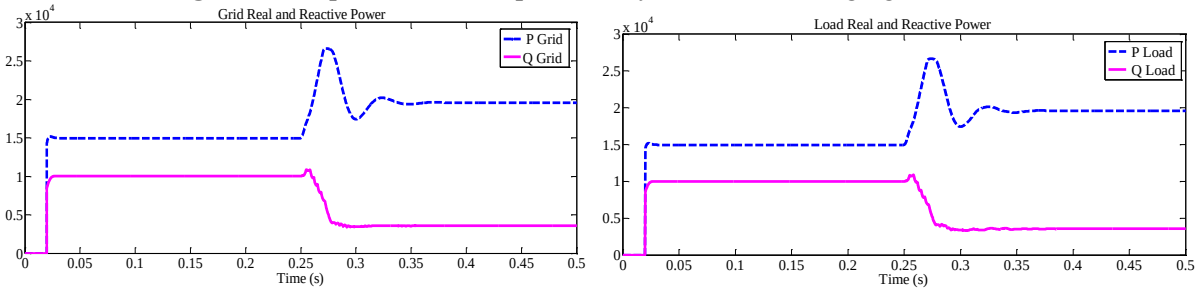

(a) (b)

Figure 4. Real and reactive power of uncompensated system under changing load conditions

5.2. Compensated System

The compensated system consists of a two-stage 25 kW three phase grid connected SPV System with linear and non-linear loads at the PCC. Decoupled control with load harmonics extraction is employed as the control scheme for the PV inverter. The performance is investigated under changing load conditions with constant irradiance of 400 W/m^2 and temperature of 25° C. Figure 5 depicts the grid and the load voltage and current waveforms under the changing load conditions. It can be seen that the grid side currents remain sinusoidal even if the load currents are distorted.

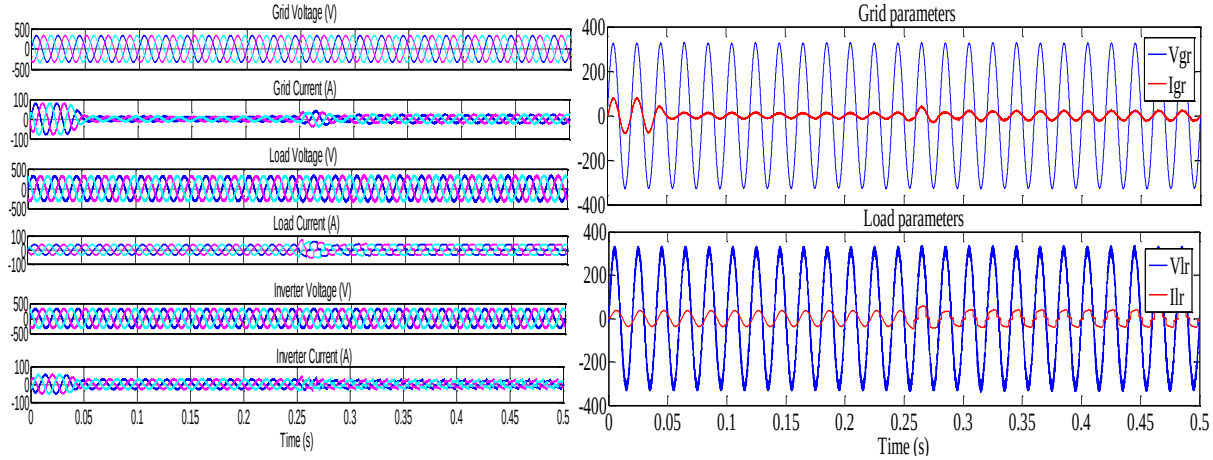

(a) (b)

Figure 5. Response of compensated SPV system under changing load conditions

Figure 6 depicts the grid, the load and the inverter real and reactive power. It can be observed that the entire reactive power requirement of the load is met by the PV inverter. Hence, the reactive power burden of the grid reduces completely and the grid power factor improves to unity. The PV inverter

also injects the available real power from the SPV system at the given conditions of temperature and irradiance to the PCC. Hence the SPV system supplies a portion of the real power requirement of the load and the grid has to supply only the remaining real power. Figure 7 shows the boost converter output voltage i.e. the dc link voltage which is regulated to the reference value V_{dcref} of 700 V by 0.8% even under changing load conditions.

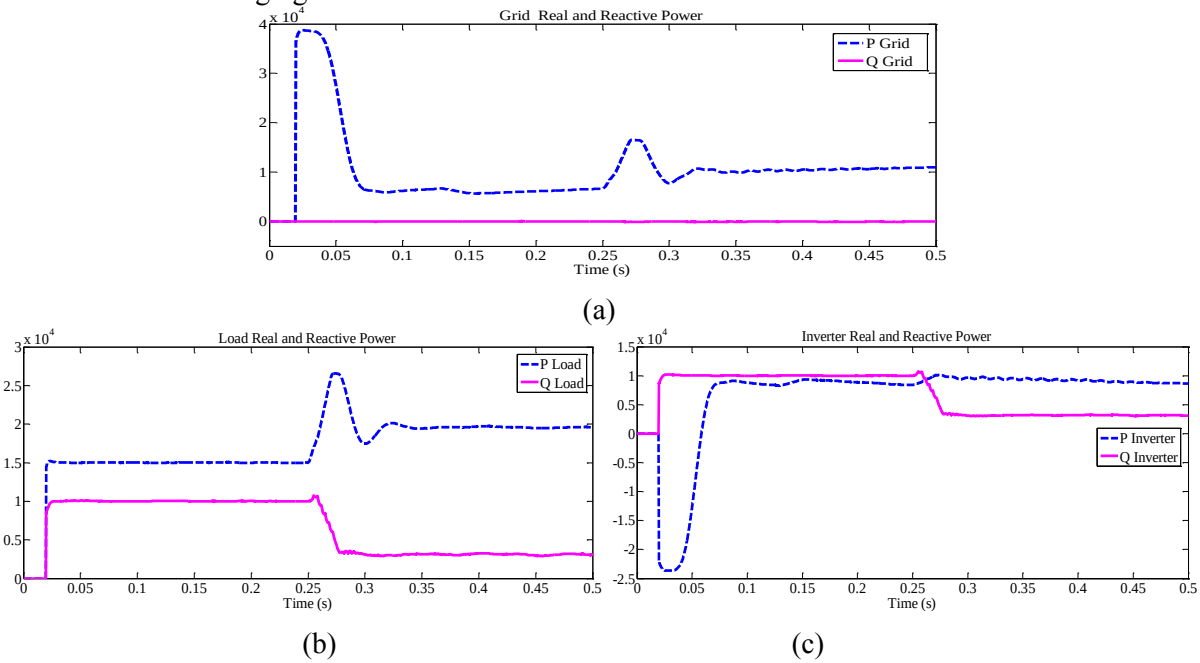

Figure 6. Real and reactive power of compensated SPV system under changing load conditions

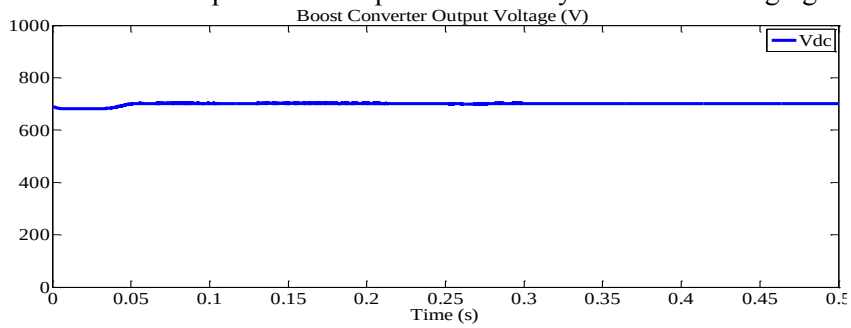

Figure 7. Voltage at the dc link of SPV system under changing load conditions

Table 3. THD Comparison.

THD (%)	Uncompensated System		Compensated System with SPV-DSTATCOM	
	Reactive Load	Reactive and Diode Rectifier Load	Reactive Load	Reactive and Diode Rectifier Load
Grid Voltage	0%	0%	0%	0%
Grid Current	0%	22.07%	1.46%	5.41%
Load Voltage	0%	0.97%	1.73%	1.67%
Load Current	0%	22.07%	0%	22.43%

Based on the simulation results, a comparison of THD values of the grid and the load voltages and currents for the uncompensated system and compensated system with SPV-DSTATCOM is given in table 3. It can be seen that the implementation of decoupled control approach with load harmonics extraction for the grid integrated SPV system causes significant reduction in the THD values of grid current even in the presence of highly non-linear loads.

6. Conclusion

In recent years, new challenges and opportunities in power quality management have emerged due to the increased penetration of DG systems based on RES and the proliferation of power electronic based non-linear loads. In an uncompensated system, the presence of non-linear diode rectifier loads at the PCC causes the grid currents to become distorted and the grid has to supply the entire real and reactive demand of the load. Also, the grid p.f. is lagging. In this work, a control strategy based on decoupled control with load harmonics extraction is developed for the grid integrated SPV system. It can be seen that the PV inverter functions as a virtual DSTATCOM and the grid current remains distortion free even with highly non-linear loads connected at the PCC.

The simulation results show that the implementation of decoupled control provides independent control of real and reactive power and regulation of the dc link voltage to the desired level. The PV inverter supplies the entire reactive power requirement of the load hence reducing the reactive burden of the grid completely and the grid p.f. is improved to unity. According to the available generated PV power at the given conditions of temperature and irradiance, the PV system provides a portion of the real power demanded by the load. Thus, the grid has to supply only the remaining real power required by the load. However, this system suffers from the drawback that the response time of the controller is more. A modification on the control strategy may give faster response under changing conditions of temperature, irradiance and load.

References

[1] Chidurala A, Saha T K and Mithulananthan N 2016 Harmonic impact of high penetration photovoltaic system on unbalanced distribution networks - learning from an urban photovoltaic network *IET Renew. Power Gener.* **10 (4)** 485–94

[2] Blaabjerg F, Teodorescu R, Liserre M and Timbus A V 2006 Overview of control and grid synchronization for distributed power generation systems *IEEE Trans. Ind. Electron.* **53 (5)** 1398–409

[3] Eltawil M A and Zhao Z 2010 Grid-connected photovoltaic power systems: technical and potential problems- a review *Renewable and Sustainable Energy Reviews* **14** 112-29

[4] Akagi H 1996 New trends in active filters for power conditioning *IEEE Trans. Ind. Appl.* **32** 1312–22

[5] Singh B, Chandra A and Solanki J 2009 A comparison of control algorithms for DSTATCOM *IEEE Trans. Ind. Electron.* **56 (7)** 2738–45

[6] Kroposki B and DeBlasio R 2000 Technologies for the new millennium: photovoltaics as a distributed resource *Proc. IEEE Power Engineering Society Summer Meeting (Seattle, WA)* vol 3 pp 1798–801

[7] Blaabjerg F, Chen Z and Kjaer S B 2004 Power electronics as efficient interface in dispersed power generation systems *IEEE Trans. Power Electron.* **19 (5)** 1184–94

[8] Esram T and Chapman P L 2007 Comparison of photovoltaic array maximum power point tracking techniques *IEEE Trans. Energy Convers.* **22 (2)** 439–49

[9] Agarwal R K, Hussain I and Singh B 2016 LMF-based control algorithm for single stage three-phase grid integrated solar PV system *IEEE Trans. Sust. Energy* **7 (4)** 1379–87

[10] Villalva M G, Gazoli J R and Filho E R 2009 Comprehensive approach to modeling and simulation of photovoltaic arrays *IEEE Trans. Power Electron.* **24 (5)** 1198–208

[11] Schauder C and Mehta H 1993 Vector analysis and control of advanced static VAR compensators *IEE Proc. C- Generation, Transmission and Distribution* vol 140 pp 299–306